Journal of Petroleum Exploration and Production Technology (2019) 9:911–925
https://doi.org/10.1007/s13202-018-0562-0

ORIGINAL PAPER - EXPLORATION GEOPHYSICS

Petrophysical characterisation of reservoir intervals in well-*X* and well-*Y*, M-Field, offshore Douala Sub-Basin, Cameroon

Gilbert M. Chongwain[1] · **Olawale Olakunle Osinowo**[2] · **Marie J. Ntamak-Nida**[3] · **S. E. A. Biouele**[4] · **Eric. N. Nkoa**[4]

Received: 26 April 2018 / Accepted: 5 October 2018 / Published online: 31 October 2018

Abstract

Studies for the characterization of hydrocarbon reservoirs using well logs have been carried out in the M-Field of the Douala Basin to evaluate the hydrocarbon prospectivity, delineate hydrocarbon zones and determine the petrophysical properties of the identified reservoir rocks. Data from two wells comprising gamma ray, resistivity, neutron, density logs were used. Gamma ray log was used for lithologic discrimination; resistivity log was employed to identify formation fluid based on electrical responses of reservoir formations, while combined density and neutron logs were used to estimate reservoir porosity, as well as ascertain hydrocarbon type where present. Four hydrocarbon bearing reservoirs were delineated in the study area; one in Well-*X* (X_2) with a thickness of 6.2 m and three others in Well-*Y* (Y_1, Y_2, Y_3) with thicknesses of 19.2 m, 7.6 m and 78.7 m, respectively. Neutron–density crossplots indicate heterogeneous reservoir matrix comprising of sand, limestone and dolomite. The reservoirs were correlated using gamma ray log and were found to be discontinuous across the wells. The petrophysical parameters of the reservoirs evaluated indicate porosity, water-saturation and hydrocarbon-saturation values of X_2 to be 20.8%, 30.8% and 69.2%, respectively, and the average porosity, water saturation and hydrocarbon saturation of the Well-*Y* reservoirs to be 40.2%, 18.3% and 81.7%, respectively. The porosity value indicates medium–high formation porosities and oil as the dominant hydrocarbon type. The crossplot of water-saturation and porosity revealed that the grain size variation of the reservoirs ranges from fine-grained to silty sands. The bulk volume water (BVW) values for the M-Field reservoirs suggest that they are homogeneous and at irreducible water saturation (Swirr) and hence will produce water-free hydrocarbons.

Keywords Douala Basin · Well log · Petrophysical properties · Reservoir description

Introduction

The M-Field is an offshore field located within the Douala Basin. The two wells of interest pseudo-named Well-*X* and Well-*Y* due to Cameroon's National Hydrocarbon Corporation (SNH) confidentiality agreement were drilled; the locations of the wells were suggested from preliminary studies carried out in this field which has an area coverage of 2800 km^2. The wells penetrated the Paleocene-Eocene N'kapa Formation which was formed during a period of renewed thermal subsidence accompanied by extensive marine deposition and thin, isolated turbidite sands. Well log derived information are useful for formation evaluation and apt at estimating hydrocarbon (oil & gas) quantities in a reservoir (Asquith and Krygowski 2004). The evaluation of reservoir rocks in terms of their porosity, water saturation and permeability determinations, enhances the ability to estimate hydrocarbon reserves and reservoir bed thickness, and to distinguish between gas, oil and water bearing strata, by observing their electrical resistivity and relative permeability value (Hilchie 1990); (Schlumberger et al. 1996); (Uguru et al. 2002). Renewed exploration activity within the Douala Basin due to the fast depletion of known resources necessitates an integral study of the two wells. Desk work study indicates that there is no academic work

✉ Olawale Olakunle Osinowo
olawale.osinowo13@alumni.imperial.ac.uk;
wale.osinowo@ui.edu.ng

1 Pan African University Institute of Life and Earth Sciences (Including Health and Agriculture), University of Ibadan, Ibadan, Nigeria

2 Departments of Geology, University of Ibadan, Ibadan, Nigeria

3 Departments of Earth Sciences, University of Douala, Douala, Cameroon

4 National Hydrocarbon Corporation (SNH), Yaoundé, Cameroon

done or published data, regarding petrophysical analysis of wells in this field, thus, the present study is aimed towards the petrophysical analysis of the rock units drilled in M-Field for evaluating the reservoir potential and establishing the stratigraphic relationship between the identified reservoirs encountered in these wells.

Geological setting

The Douala/Kribi-Campo Basin located in the northern end of the South Atlantic is one of a series of divergent passive margin basins along the west coast of Africa, covering a total area of 19,000 km^2 including 7000 km^2 area

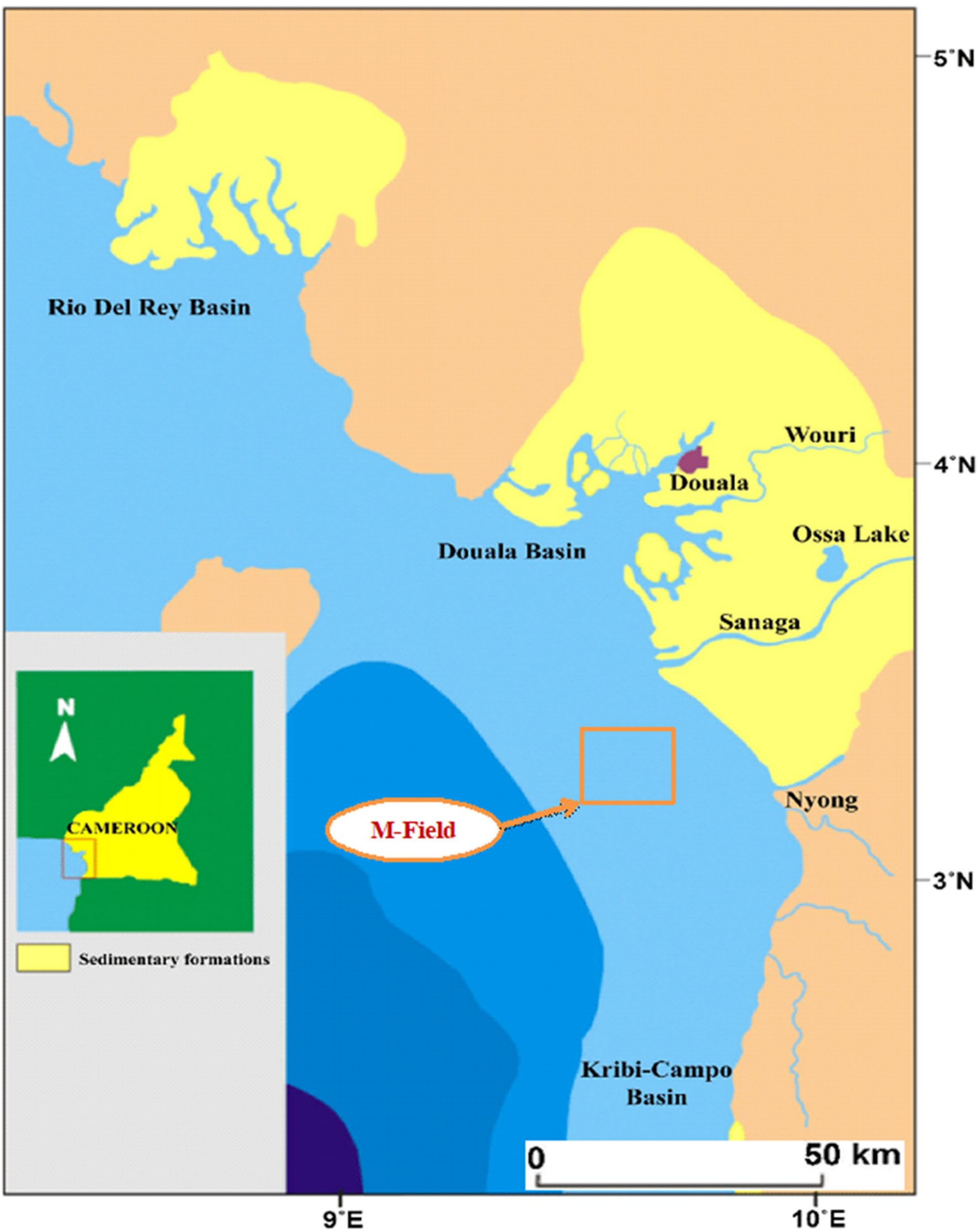

Fig. 1 Location map of the study area

which is located onshore (Pauken et al. 1991). The study area is located offshore and falls within the PH77 Prospect (Fig. 1). The deposits of this basin range from Cretaceous to Recent, the stratigraphy, as well as the sedimentology has been described in detail by Brownfield and Charpentier (2006) and Ntamak-Nida et al. (2010), respectively. Eight litho-stratigraphic units which comprises the Mundeck, Logbadjeck, Logbaba, N'kapa, Souellaba, Kribi (Unnamed), Matanda and Wouri formations have been identified (Fig. 2). The N'kapa Formation which is the formation of interest in this study was deposited during the Palaeocene with no evidence of fault reactivation associated with the extension of the Atlantic during the Eustatic sea level changes which resulted in the subsidence and extensive deposition of marine sediments in neighbouring basins. The N'kapa Formation represents the top package of the Megasequence B (Manga 2008) and comprises mainly of silty mudstones and argillaceous sandstones which indicate muddy shelf environment. The reservoirs are mainly deep-water (including turbidite) with sand porosities ranging between 22 and 30% and permeability value less than 32mD (Simon Petroleum Technology (SPT) 1995). The formation is characterized mostly by stratigraphic trap (syns-sedimentary) mounds and sand sheet, as well as sub-unconformity traps formed beneath the Souellaba Formation Mid-Oligocene unconformity.

Materials and methods

This study utilized wireline log data to qualitatively and quantitatively determine the petrophysical properties of reservoir intervals using Senergy Interactive Petrophysics (IP.v, 3.6) software. Well logs which record different physical borehole parameters against depth were interpreted and subjected to various petrophysical analyses and also employed to carry out litho-stratigraphic correlation across the wells. Through this the distribution and behaviour of the lithological units of interest across different well locations were established. Measured log parameters including gamma ray, resistivity, density, neutron, sonic among others were employed to qualitatively identify porous and permeable litho-units which are hydrocarbon saturated and possess right qualities that distinct them as hydrocarbon reservoirs. The well log information were also employed to quantitatively determine other derivative reservoir parameters such as, reservoir thickness, Net-To-Gross (NTG), volume of shale (V_{sh}) in the reservoirs,

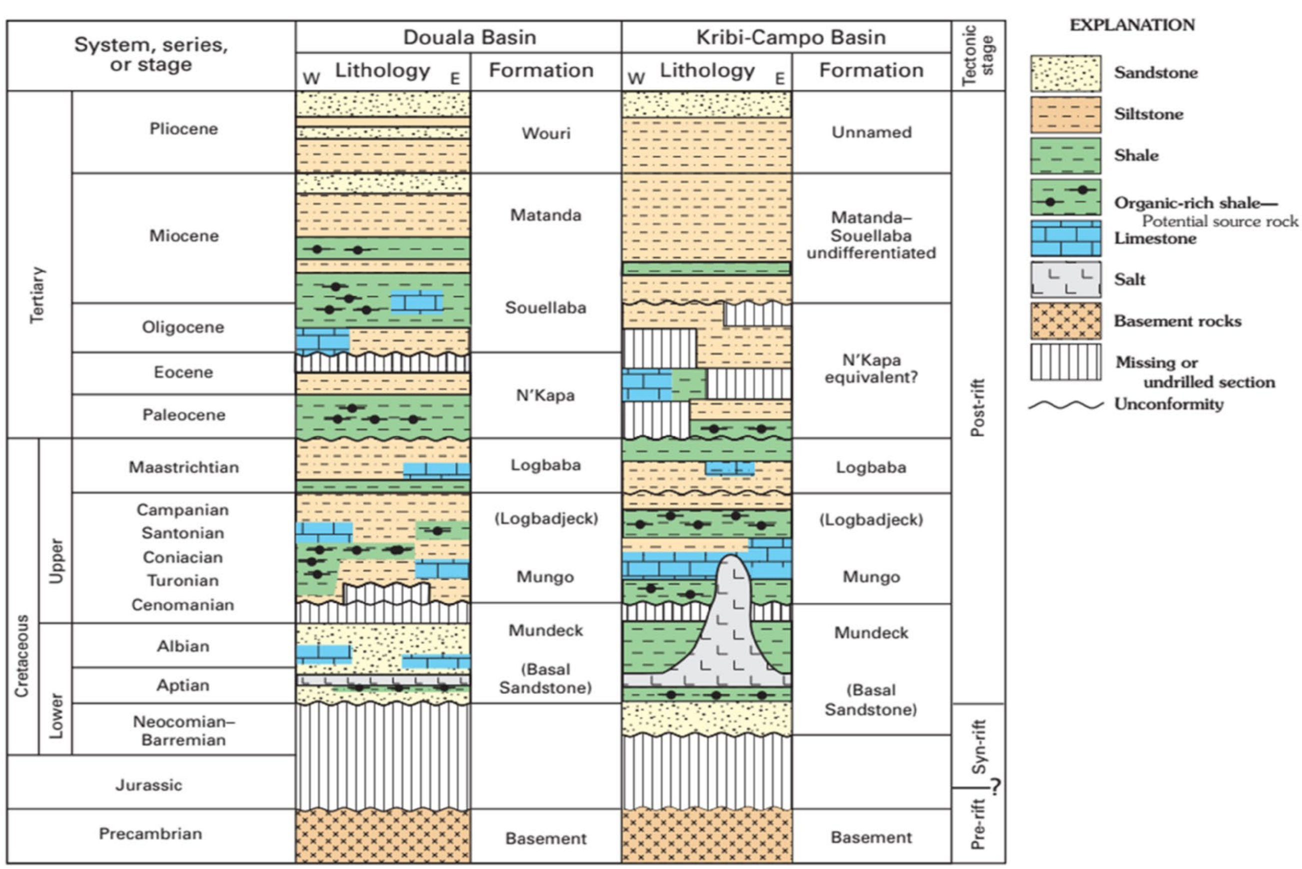

Fig. 2 The stratigraphy of the Doula Basin and Kribi-Campo Basin (Brownfield and Charpentier 2006)

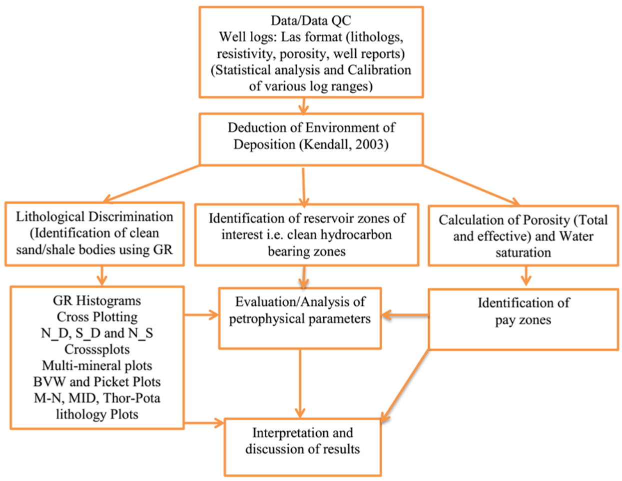

Fig. 3 Simplified workflow adopted to characterize M-field, offshore Douala Sub-Basin, Cameroon

effective porosity (Ø_{eff}) and hydrocarbon saturation (1-S_w) which were used to evaluate the hydrocarbon potential of M-field. Figure 3 presents the workflow which summarizes the different activity steps embarked upon to characterize M-Field, Douala Sub-Basin, Cameroon.

The Gamma ray logs for the two wells were normalized based on the method and guidelines reported by (Shier and I2 FIGURES 2004) and were employed to identify the reservoir units; a shale cut-off value of 60 was used for both wells *X* and *Y*, to establish the sand base line and thus discriminate reservoir units based on the lower GR readings (Fig. 4). In addition, to enable accurate reservoir lithologic description relevant for reservoir management, Sonic–Density, Neutron–Density, Neutron–Sonic, M–N crossplots, as well as mineral identification (MID) plots were further employed to determine reservoir lithology and associated constituent rock minerals. The fields of plots of the log values on the crossplots which were generated using IP software enabled the ease of accurately determining reservoir lithologies and constituent mineralogy. The fluid within the delineated reservoir units, as well as the oil–water Contact (OWC) was differentiated using a combination of deep (AHT90), medium (AHT60) and shallow (AHT30) resistivity logs capable of measuring formation resistivity of the flushed, transition and un-invaded zones around the well bore environment. The deep resistivity (AHT90) was used to identify hydrocarbon bearing zones; zones with resistivity values greater than 4 Ω-m were identified as hydrocarbon bearing (track 4 in Fig. 4) as low resistivity pay hydrocarbon zones have been widely reported within resistivity ranges of 4 Ω m, especially within fine grain lithologies (Afizu 2013). The deep resistivity log in combination with the GR log were used to differentiate between hydrocarbon and non-hydrocarbon bearing zones and consequently defined the zones of interest in terms of clean sands saturated with hydrocarbon (low GR and high resistivity). GR histograms were produced for each reservoir and the clustering pattern observed to infer the extent of cleanliness of the reservoir (Goncalves et al. 1995) (Fig. 5). The neutron compensation porosity log corrected for all except for formation water salinity (TPHI) and the bulk density porosity log (RHOZ) were used together to discriminate the hydrocarbon types (whether oil or gas) present in the reservoirs (track 5 in Fig. 4a). The characteristic "Balloon effect" usually associated with the underestimation and overestimation of gas by neutron and density logs, respectively, within a gas saturated reservoir served as a guide. Further characterisation of Well *Y* reservoirs was not possible because of the absence of density logs to compute the porosities.

The clay volume (V_{clay}) within the delineated reservoir unit was also estimated for ease of estimating effective porosity, using the computed gamma ray curve (CGR), this was carried out using the Larionov Tertiary Eqs. 1 and 2 (Asquith and Krygowski 2004) as the N'kapa Formation is Tertiary in Age (Brownfield and Charpentier 2006) and the general aspects of the curves indicated possible thin laminated reservoirs. The interpreted plots were subsequently presented using dispersed, laminated and structural shale on the lithological tract.

Linear response (Vcclay = IGR):

$$\text{VclGr} = \text{IGR} = \frac{\text{Gr} - \text{GrClean}}{\text{GrClay} - \text{GrClean}} \tag{1}$$

The Larionov younger rocks nonlinear responses for Tertiary rocks (Larionov 1969)

$$\text{VclGr} = 0.08336(2^{3.7xZ} - 1)$$

$$Z = \text{VclGr} \tag{2}$$

The Density–Porosity Model which captures the empirical relationship that relates the measured bulk density (ρ_b), porosity (Φ), matrix (ρ_{ma}) and fluid (ρ_f) densities while integrating the clay volume effect was used to determine formation fractional porosity (Eq. 3). A cutoff of 15% based on the geological characteristics of the N'kapa Formation and other formations in the Douala Basin was adopted, thus formation fractional porosity value higher than 15% were considered zone of interest.

$$\text{Ø} = \frac{\left(\rho_{ma} - \rho_b - V_{cl} \times \left(\rho_{ma} - \rho_{cl}\right)\right)}{\rho_{ma} - \rho_f \times S_{xo} - \rho_{HyAp} \times \left(1 - S_{xo}\right))} \tag{3}$$

where ρ_{ma} = matrix density; ρ_b = input bulk density log; cl = wet clay density; ρ = filtrate density; ρHyAp = apparent hydrocarbon density; V_{cl} = wet clay volume and S_{xo} = flushed zone water saturation.

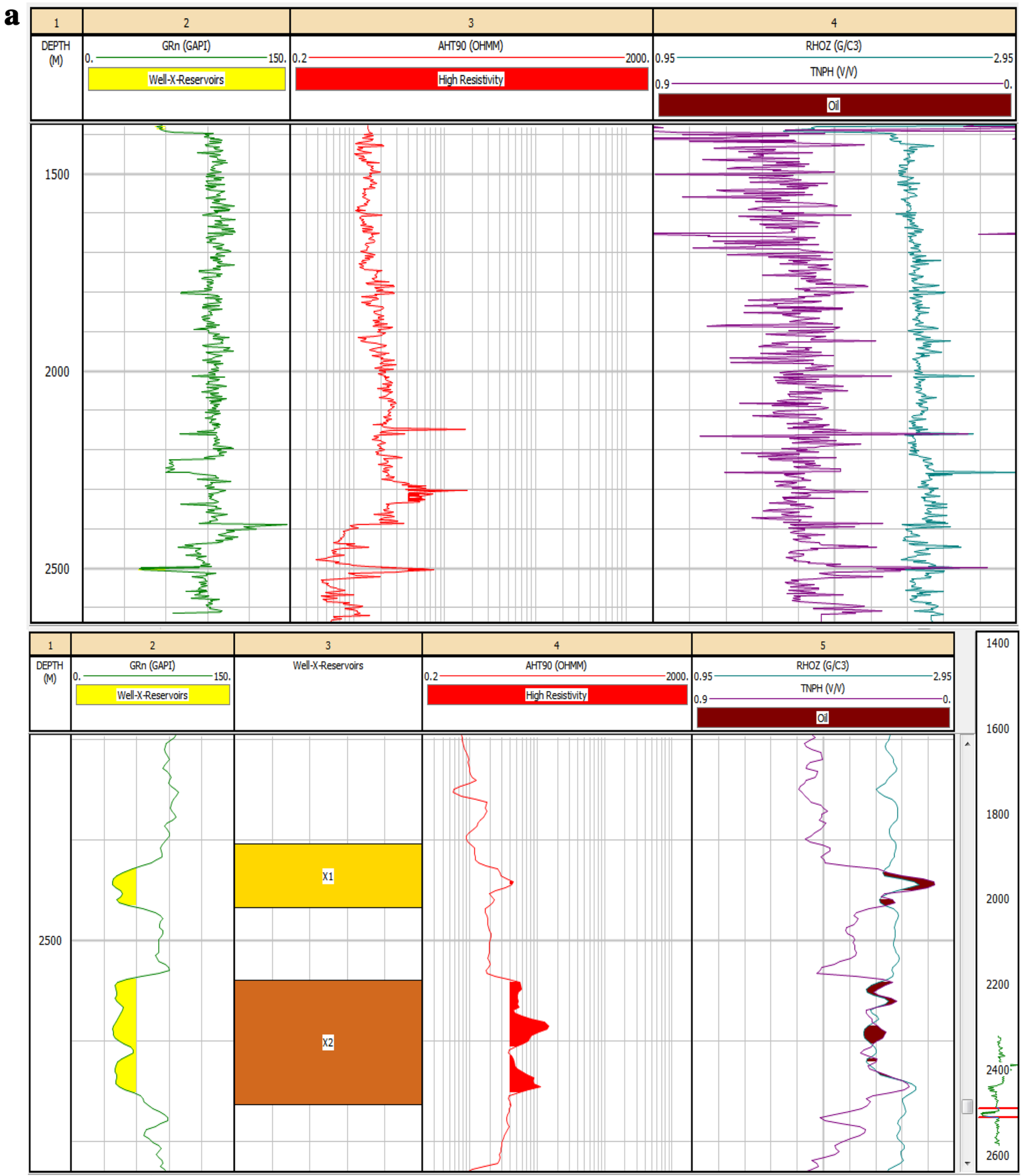

Fig. 4 **a** Well log signatures of studied interval in Well X and the identified reservoirs (X_1 and X_2). **b** Well log signatures of studied interval in Well Y and the identified reservoirs (Y_1, Y_2 and Y_3)

Water saturation (S_w) which signifies the fraction or percentage of pore space that is occupied by water (Holstein and Warner 1994) was determined for the identified reservoir units based on the Simandoux water saturation formula (Eq. 4) which took into consideration the impact of the clay volume. This enabled the ease of determining

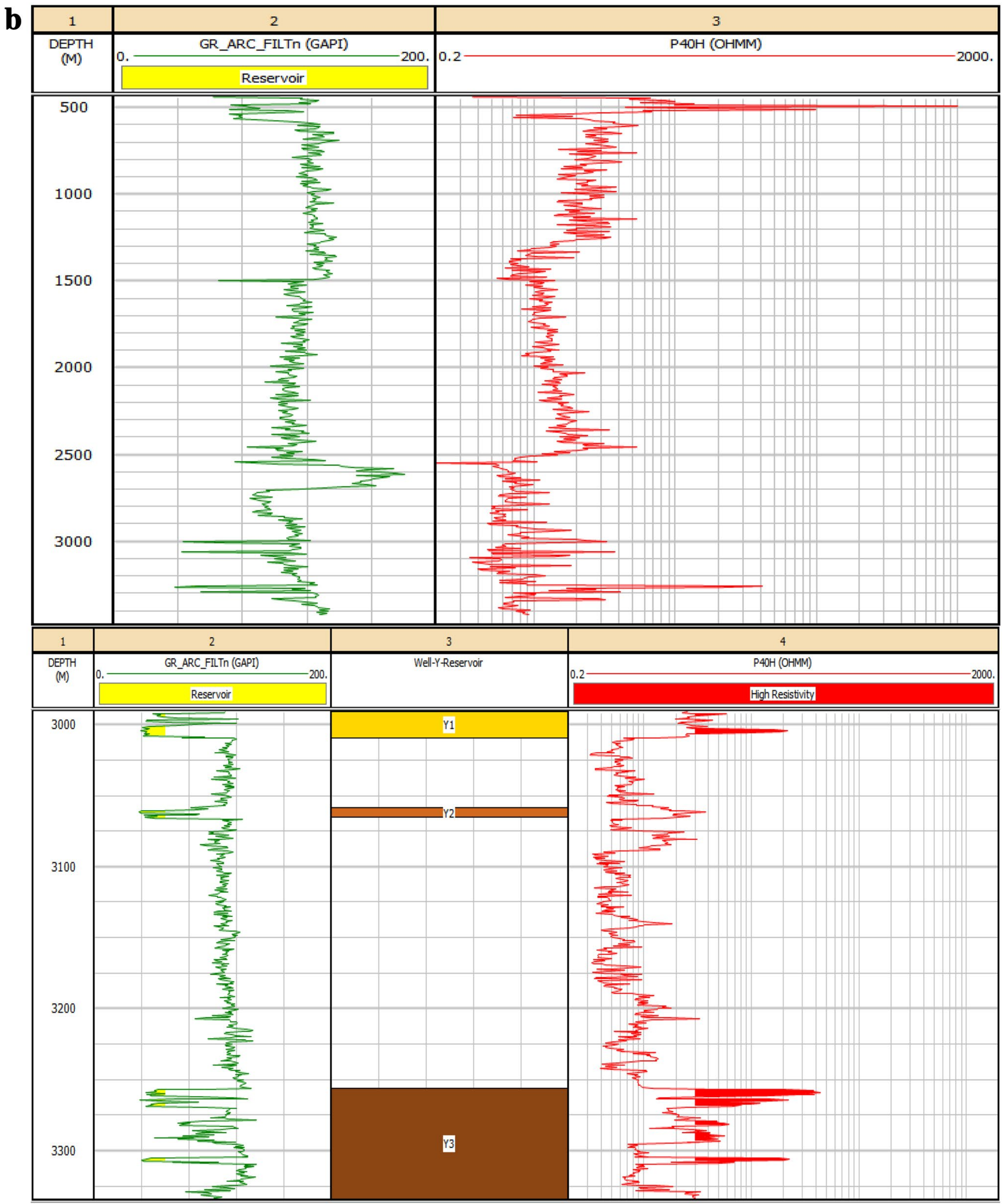

Fig. 4 (continued)

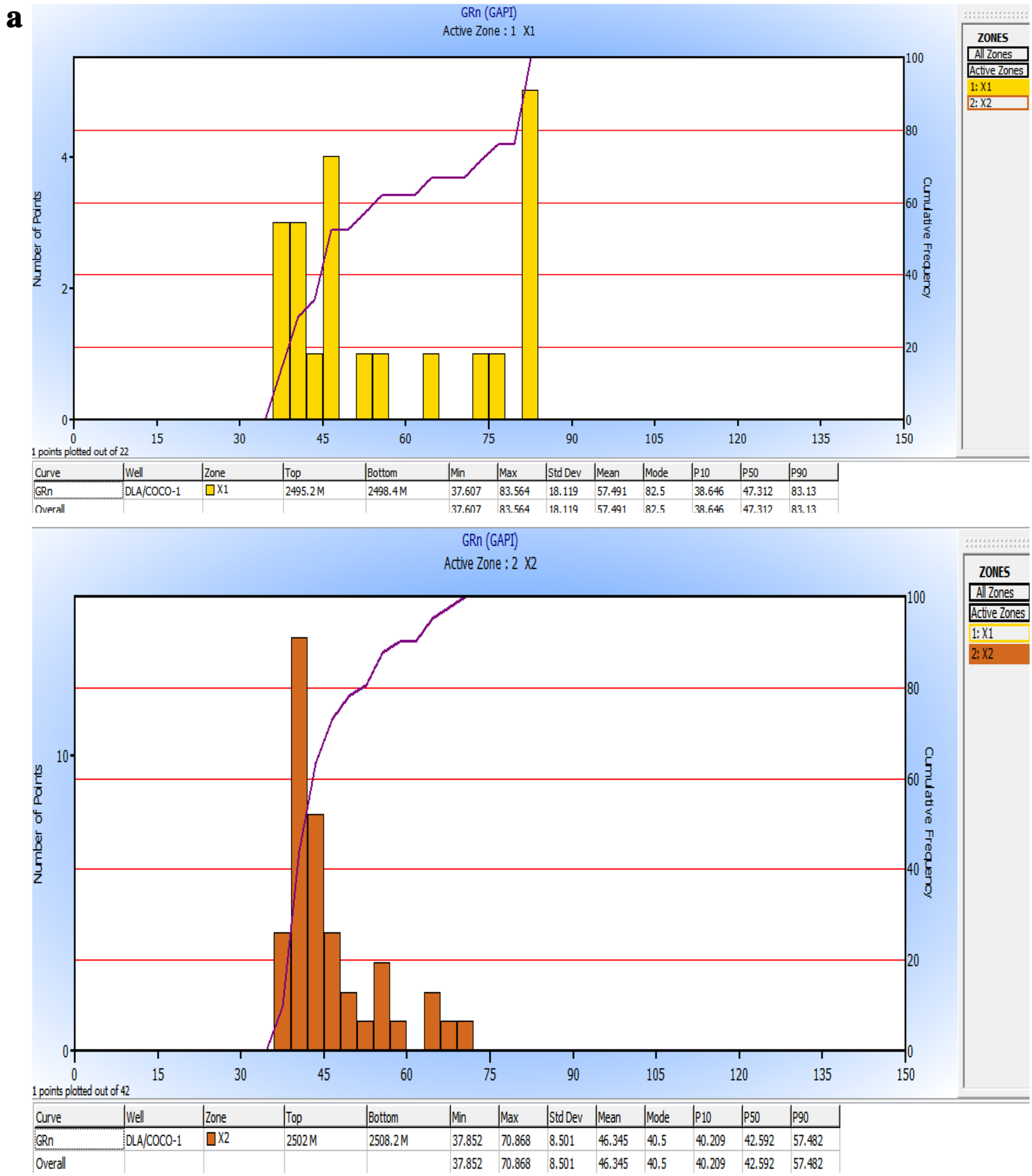

Fig. 5 **a** GR_Histogram for Well X reservoirs showing considerable points plotting beyond 60API in X_1 and most points clustering below 60 API in X_2 revealing that X_2 is clean relative to the dirty X_1 in terms of clay content. **b** GR_Histogram for Well-Y reservoirs showing considerable points plotting beyond 60API in Y_1, Y_2 and Y_3 revealing that Y_1 and Y_2 are clean relative to the dirty Y_3 in terms of clay content

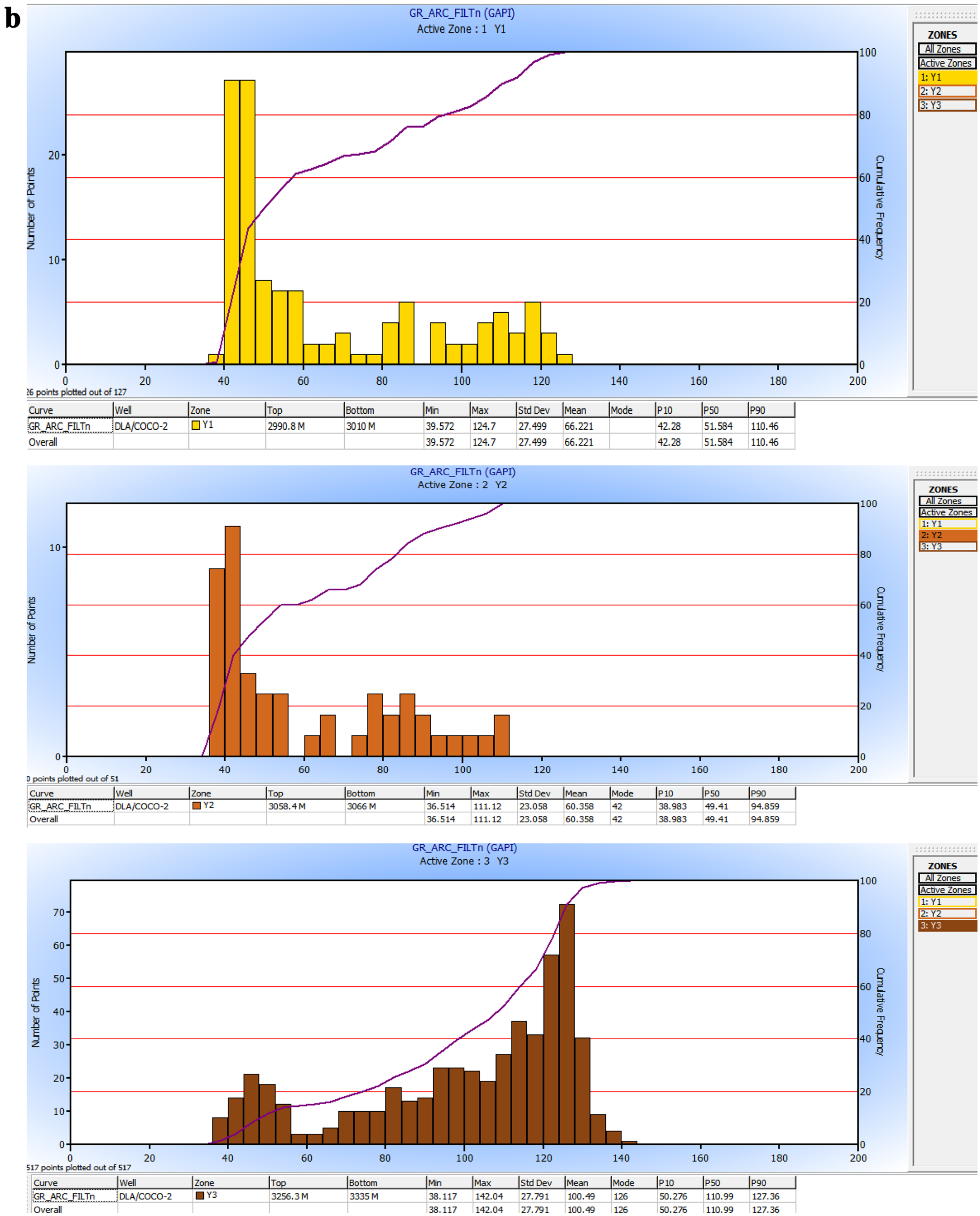

Fig. 5 (continued)

hydrocarbon saturation (Eq. 5) and subsequently the volume of hydrocarbon initially in place.

$$\frac{1}{R_t} = \frac{\emptyset^m \times S_w{}^n}{a \times R_w} + \frac{V_{cl} \times S_w}{\mathrm{Rcl}} \quad (4)$$

where, R_w = water resistivity; R_t = true formation resistivity; a = tortuosity factor; m = cementation factor; $\varnothing$ = formation porosity, S_w = effective water saturation; V_{cl} = wet clay volume and Rcl = resistivity of the clay.

Then using Eq. 5 below, the Hydrocarbon Saturation for the reservoir zone was computed.

$$S_h = 1 - S_W \text{ or } S_h = 100 - S_W(\%) \quad (5)$$

where, S_h = Hydrocarbon Saturation; S_W = Water Saturation.

Bulk volume water (buckle plots)

Finally, bulk volume water (BVW) which is a product of the formation water saturation (S_w) and its porosity ($\varnothing$) (Eq. 6) was used to estimate the reservoir formation grain size through the use of comparative chart described by (Holstein and Warner 1994).

$$\mathrm{BVW} = S_w\, x\, \emptyset. \quad (6)$$

Results and interpretation

This section presents the qualitative and quantitative reservoir parameters such as lithologic properties, reservoir intervals, volume of shale, porosity, saturation and permeability as encountered in the two wells. The obtained results are presented as Well log responses, lithologic sections, cross plots, tables among others.

Reservoir identification and evaluation

Five reservoir units were identified based on the GR log response of the two wells. In Well X, two reservoir bodies were identified including X_1 encountered between 2495 and 2498.3 m, while the second X_2, was encountered between 2502 and 2508.2 m with gross thicknesses of 3.2 m and 6.2 m respectively (Fig. 4a), while for Well Y, three reservoir bodies were delineated including Y_1, Y_2 and Y_3 with gross thicknesses of 15.1 m, 6.4 m and 37.8 m respectively (Fig. 4b). Further analysis of resistivity log data indicates that all the reservoirs in both Well X and Y are hydrocarbon bearing due to their high resistivity responses. A crossplot of the neutron and density logs for X_1 and X_2 reservoirs showed no observable "balloon effect" suggesting the occurrence of oil as the hydrocarbon phase and this was further supported by a hydrocarbon density of 0.8 exhibited by reservoir X_2. However, X_1 contains no producible hydrocarbons in Well X (i.e. no pay zone) though with low GR readings and high resistivity readings and this is characteristic of calcareous interbeds which usually show unique characteristics of low natural gamma (less than 80 API) and higher lateral resistivity than any other sandstone (Zhu et al. 2018). There are four common types of calcareous interbeds (Sun et al. 2010); (Zhang et al. 2007); (Wang et al. 2009); (Zhang et al. 2009); (Qi et al. 2006) and the X_1 reservoir possibly typifies the complete type calcareous interlayer in which the isolated thin sand layer was wrapped in mudstone and the entire sand was completely cemented by carbonate resulting in a tight reservoir (Fig. 4). Reservoirs X_2 contain oil with an average hydrocarbon saturation of 69% and a net-to-gross of 0.88 (Table 1). Also, the average volume of clay (Vclay) value of 0.10 v/v is below the damaging limits of 0.15 v/v (Hilchie 1978). The average porosity for the hydrocarbon bearing reservoir is 26%, with a permeability of 104.65 md, hence, the reservoir has very good porosity and good permeability as well (Table 2).

N–D crossplots, M–N lithology plots and THOR–POTA plots for clay typing

Neutron–Density and Sonic–Density crossplots for the Well-X reservoirs plotted uneven within all lithological fields indicating heterogeneous lithologies (i.e. DOL, LST and SS) (Fig. 6). Well-Y lacked sonic and neutron logs hence crossplots could not be produced. The M–N lithology plots depict most of the points plotting in the dolomite and calcite field (Fig. 7) and the Thorium–Potassium plot plotted mostly within the chlorite field (Fig. 8), hence the dominant clay mineral is chlorite and montmorilorite.

Clay content, porosity, water saturation and pay zone summary

The clay content, water saturation, porosity values, as well as the pay zones for the various reservoirs were plotted graphically and are presented in Fig. 9 revealing the reservoir zones (green colour) and the pay zones (red colour) of the X_2 reservoir. Petrophysical parameters of all the reservoir zones have been summarized in Table 1.

Bulk volume water (BVW or Buckle) plots

The crossplot of water-saturation (S_w) versus porosity (Ø) for reservoirs X_2, indicate that the grain size variation of the reservoirs ranges from fine-grained to silty sands (Fertl and Vercellino 1978), (Table 2). The bulk volume water plots (Fig. 10) depicts that the reservoirs are homogeneous and thus are at irreducible water saturation (Swirr), thus will produce water-free hydrocarbons.

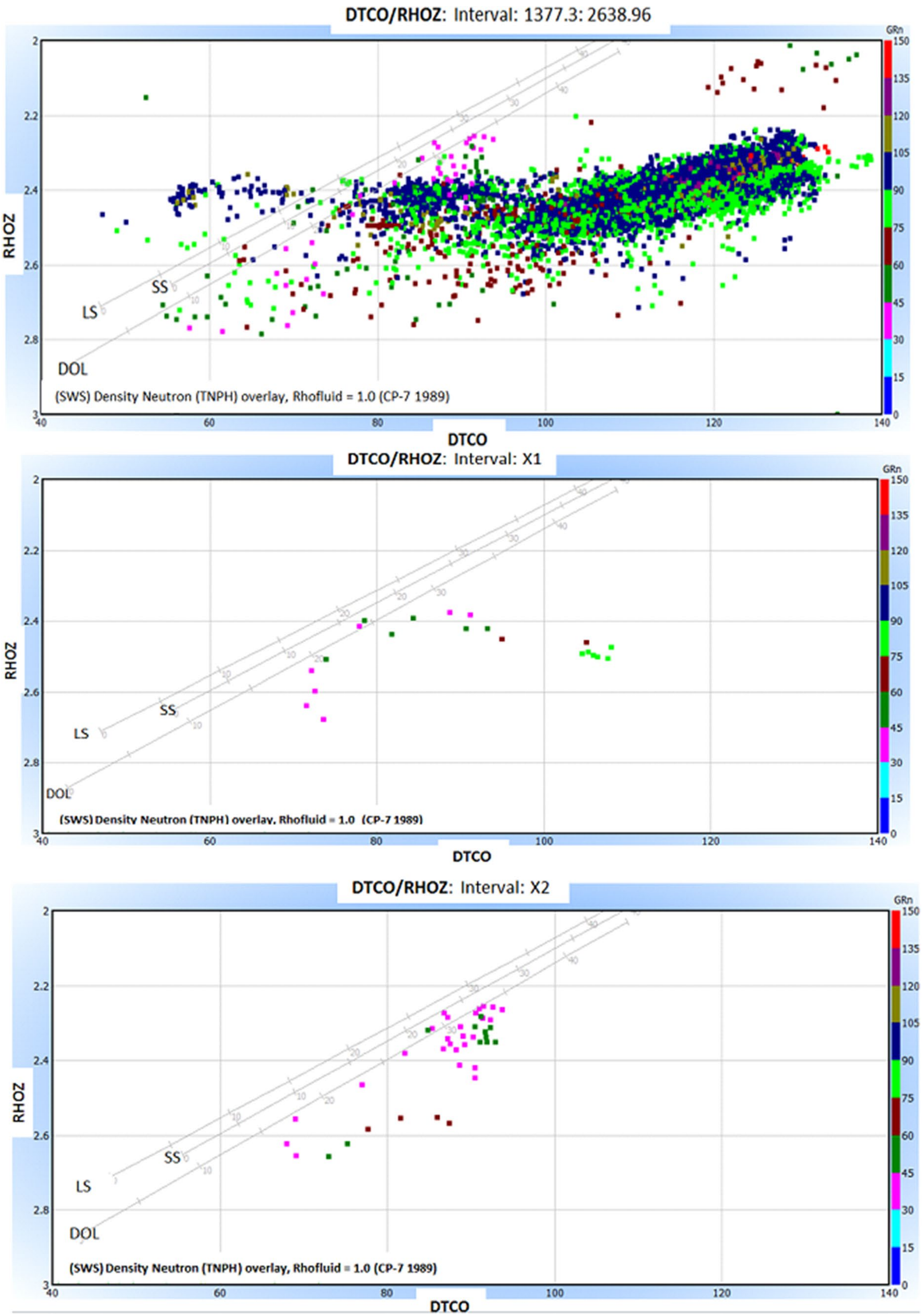

Fig. 6 Sonic–Density Crossplots for Well-*X* reservoir showing points scattered across the various fields indicating the heterogeneous nature of the reservoirs

Table 1 Summary of average petrophysical values for Well-*X*-Reservoirs of M-Field

Well-*X* reservoir	Top	Bottom	Gross	Net	N/G	AvPhi	AviSw	AvVcl	So	Perm	BVW
X_1	2495.2	2498.4	3.2	—	—	—	—	—		—	—
X_2	2502	2508.2	6.2	5.49	0.88	0.26	0.31	0.10	0.69	104.65	0.06

Table 2 Qualitative Interpretation of petrophysical properties (Zhang et al. 2007) for Well-*X*-Reservoirs of M-Field

Well-*X*-reservoirs	Bulk volume water (BVW) Fertl and Vercellino (1978)		Porosity (%) Rider (1986)	Permeability (md) Rider (1986)
	Grainsize (mm)	Reducibility		
X_1	—	—	—	—
X_2	(0.0636) Very fine	Irreducible water	(26) Very Good	(104.65) Good

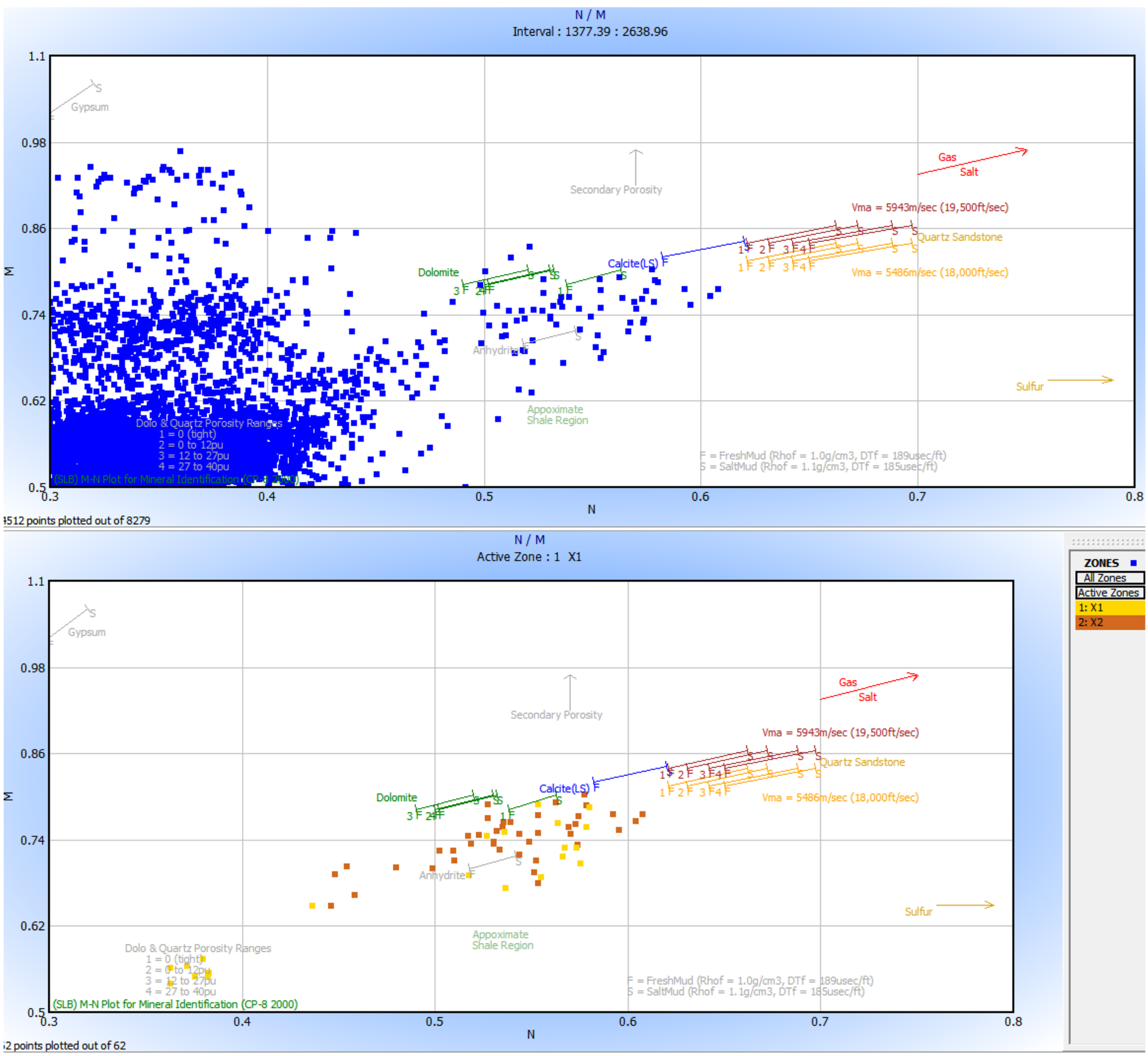

Fig. 7 M–N Lithology Plots for Well *X* reservoir interval with most of the points plot within the dolomite and calcite fields

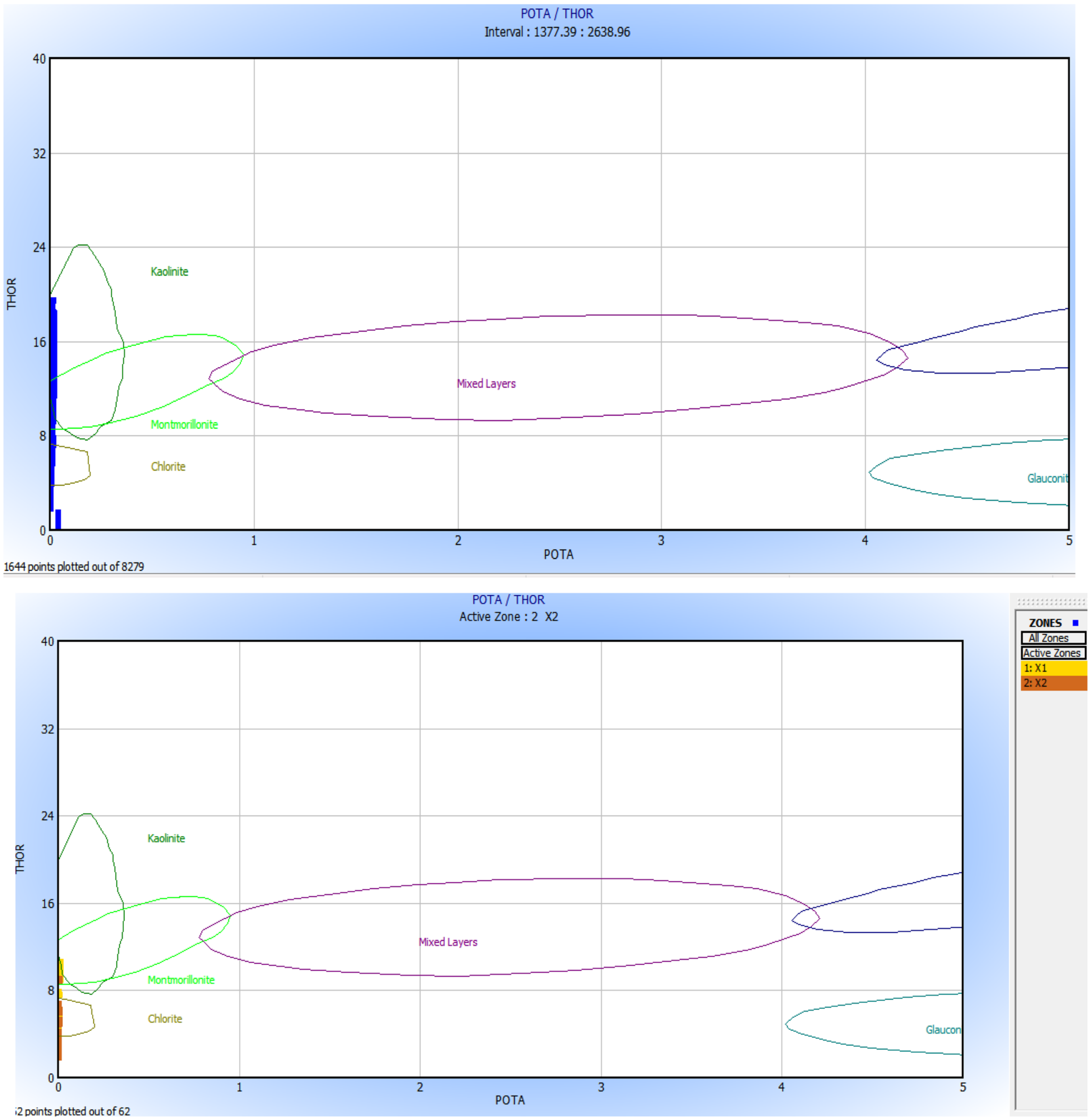

Fig. 8 Thorium–Potassium Plot for X_2 with most of the points plotting in the chlorite field and a few plotting in the montmorillonite field

Discussion

The reservoirs in the study area could be described as calcareous quartz siltstones/sandstone within the N'kapa Formation due to the heterogeneous matrix which consists of fine-grained sand, limestone and dolomite. Petrophysical evaluation carried out on the wireline logs indicate four (4) reservoirs which are discontinuous and non correlatable across the entire wells. The identified reservoirs are probably thin stratigraphic sand beds which thin out and were deposited either as channel sands or as short turbiditic events characterizing the N'kapa Formation. All the reservoirs are hydrocarbon bearing with oil as the available phase in reservoir X_2 as suggested by the absence of the balloon effect and a density of 0.8. The reservoirs identified from petrophysical evaluation are discontinuous and non correlatable

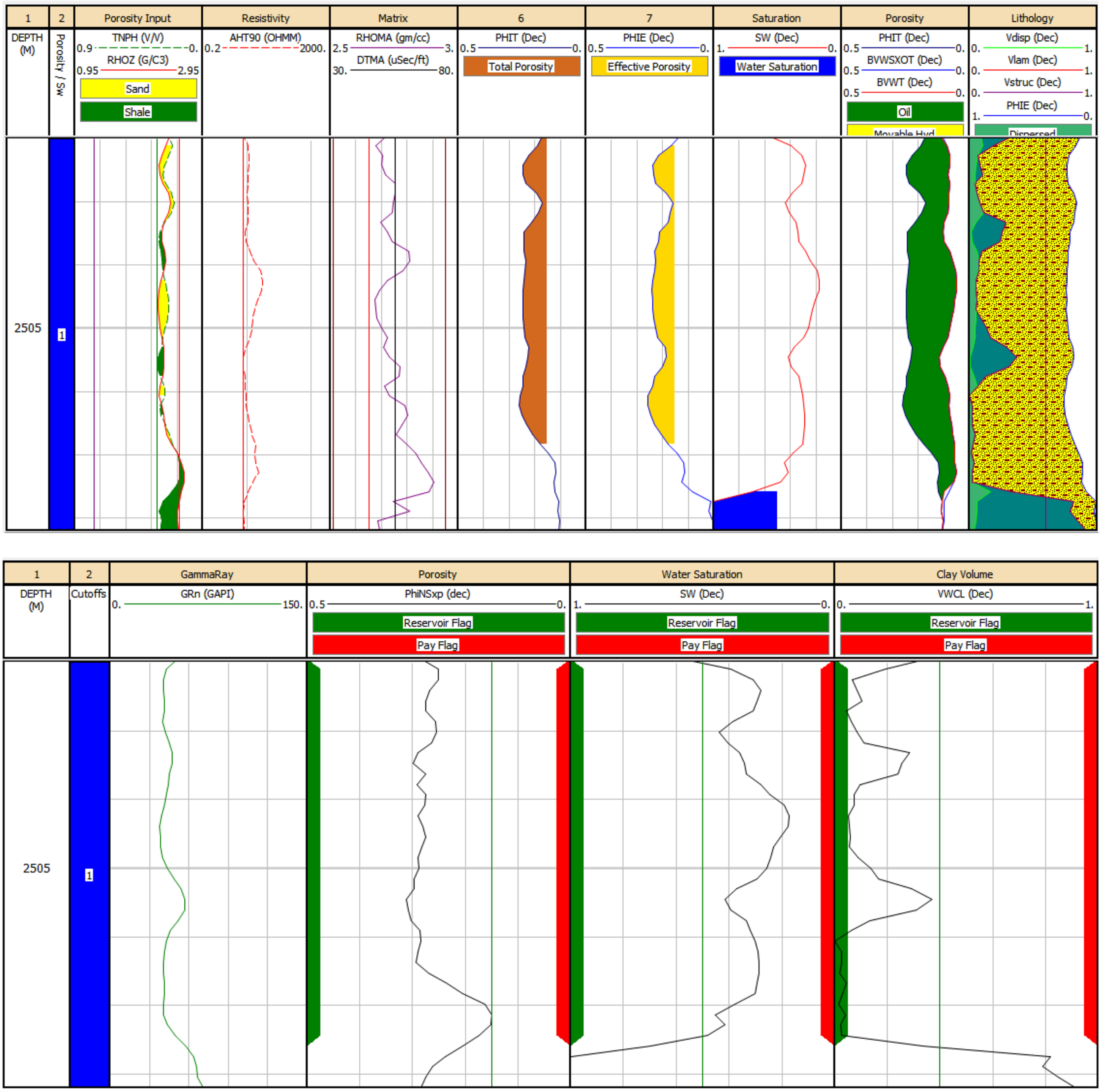

Fig. 9 Petrophysical and Pay zone summary graphical representation of X_2 reservoir

across the entire wells. They present average porosities, hydrocarbon-saturation and permeability in excess of 20%, 69% and 76 md, respectively, suggesting favourable petrophysical parameters for hydrocarbon accumulation and preservation based on the classification of (Rider 1986). They are probably thin stratigraphic carbonate prone sandy beds pinch-outs that were deposited either as channel sands or as short turbiditic events typical of the N'kapa Formation (Simon Petroleum Technology (SPT) 1995). The bulk volume water (BVW) values indicate that formation grain size ranges from fine grained to silty sands. BVW values calculated and plotted on crossplot as established by Asquith and Gibson (1982) are constant or closed to constant and parallel to the hyperbolic lines, thus suggesting that the reservoir are homogeneous and are at irreducible water saturation (Swirr) and hence will produce water-free hydrocarbon. When a reservoir is at Swirr, water will not move because it is held on grains by capillary pressure (Morris and Biggs 1967). Hydrocarbon production from a reservoir at Swirr should be water-free (Asquith and Krygowski 2004). The chlorite

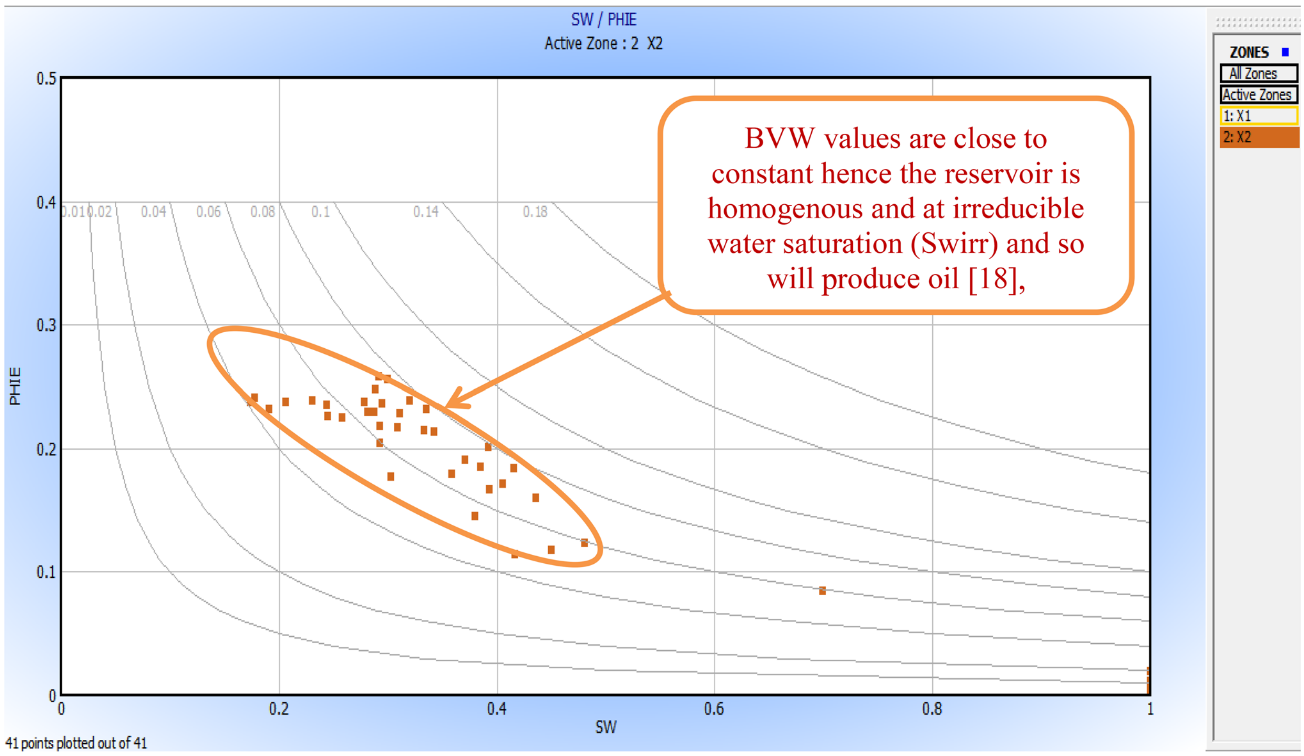

Fig. 10 Porosity versus Water Saturation plot for Reservoir X_2 showing the constant or close hyperbolic pattern which indicates that the reservoir is at irreducible water saturation

mineral could either be linked to detrital chlorite influx from neighbouring river sediments during fast deposition and/or probably formed diagenetically during early diagenesis of feldspar and mica sediments on the sea floor.

Conclusion

The petrophysical analyses performed in this study shows that the reservoir sand units of M-Field contain significant hydrocarbon accumulations within the delineated generally thin and non-correlative reservoir sands. Oil is seen as the dominant hydrocarbon type and analysis shows that the grain size is fine grained. Four prospects namely, X_2, Y_1, Y_2 and Y_3 with thicknesses of 6.2 m, 19.2 m, 7.6 m and 78.7 m, respectively, were identified as having significant hydrocarbon saturation, as well as possess good petrophysical qualities favourable for hydrocarbon accumulation, preservation and generation. The prospects as compared to the intervals identified within the N'kapa Formation are promising with fair–significant hydrocarbon potential within the Douala Basin that can be fully developed. Additionally, the mineral identification cross-plots show that the reservoirs are lithological heterogeneous consisting of fine grain matrix mainly of calcite, dolomite and subordinate quartz. Based on the evidence presented in this study, calcareous interlayers interpreted as calcareous tight reservoirs also characterize the N'kapa Formation as is the case with reservoir X_1 and searching for large-scale traps without calcareous interlayers could improve drilling success. Further calibration of the log analysis parameters with core and production data is necessary to verify the calculated values, as the permeabilities for some of the reservoir sand units are yet to be characterized.

Acknowledgements The authors acknowledge the African Union Commission (AUC) for providing funds to support this project and the Ministry of Mines, Industry and Technological Development (MINMIDT); and National Hydrocarbon Corporation (SNH), Yaoundé, Cameroon for providing research data. The invaluable suggestions of all the reviewers which helped improved the quality of this work, are greatly acknowledged.

References

Asquith G, Gibson C (1982) Basic well log for geologists. American Association of Petroleum Geologist, Tulsa Methods in Exploration, p 216

Afizu M (2013) Determining the relationship between resistivity, water and hydrocarbon saturation of rock formation using composite well logs. Acad J Interdiscip Stud 2(13):119

Asquith G, Krygowski D (2004) Basic well log analysis. AAPG methods in exploration series, vol. 28. American Association of Petroleum Geologists, Tulsa, p 244

Brownfield ME, Charpentier RR (2006) Geology and total petroleum systems of the west-central coastal province (7203), West Africa: US geological survey bulletin 2207-B, p 52

Fertl WH, Vercellino WC (1978) Predict water cut from well logs, in practical log analysis, part 4. Oil Gas J (May 15, 1978–Sept 19, 1979)

Goncalves CA, Harvey PK, Lovell MA (1995) Application of a multilayer neural network and statistical techniques in formation characterization. In: SPWLA 36th annual logging symposium, Paris, France, 26–29 June 1995, Society of Petrophysicists and Well Log Analysts, Houston, paper FF, p 1–12

Hilchie DW (1978) Applied openhole log interpretation. D.W. Hilchie Inc, Goldon, p 161

Hilchie DW (1990) Wireline: a history of the well logging and perforation business in the oil fields. D. W. Hilchie Inc., Boulder, pp 25–86

Holstein ED, Warner HR (1994) "Overview of water saturation determination for the ivishak (sadlerochit) reservoir, prudhoe bay field," paper SPE 28573 presented at the 1994 SPE annual technical conference and exhibition, New Orleans, 25–28 September

Larionov VV (1969) Radiometry of boreholes (in Russian). NEDRA, Moscow

Morris RL, Biggs WP (1967) Using log-derived values of water saturation and porosity: soc. professional well log analysts, 8th Ann Logging Symp Trans, paper O

Manga CS (2008) Stratigraphy, structure and prospectivity of the southern onshore Douala Basin, Cameroon, central Africa. Afr Geosci Rev 1:13–37

Ntamak-Nida MJ, Bourquin S, Makong JC, Baudin F, Mpesse JE, Ngouem CI, Komguem PB, Abolo GM (2010) Sedimentology and sequence stratigraphy from outcrops of the Kribi-Campo Sub-Basin: lower mundeck formation (lower cretaceous, Southern Cameroon). J Afr Earth Sci 58(1):1–18

Pauken RJ, Thompson JM, Schuman JR, Cooke JC (1991) Geology of the Douala Basin, offshore Cameroon. Am Assoc Petrol Geol Bull, 75, 3, pp. 651–652

Qi B-W, Lin C-M, Qiu G-Q, Li Y-L, Liu H-M, Gao Y-J (2006) Formation mechanism of calcareous incrustation in lenticular sandbody of the shahejie formation of paleogene and its influence on hydrocarbon accumulation in Dongying Sag. J Palaeogeogr 8:519–530

Rider M (1986) The geological interpretation of well logs. Blackie, Glasgow, pp 151–165

Simon Petroleum Technology (SPT) (1995) Petroleum geology and hydrocarbon potential of the Douala Basin, Cameroon Unpubl. non-exclusive report

Schlumberger C, Schlumberger M, Leonardon EG (1996) Log Interpretation Chart Book, Schlumberger Well Surveying Corporation, Houston, pp. 201

Shier DE (2004) Petrophysics. Vol. 45. No. 3 (May–June 2004); p 268–280; I2 figures. Petrophysics, 45, 268

Sun Z-X, Sun Z-L, Lu H-J, Yin X-J (2010) Characteristics of carbonate cements in sandstone reservoirs: a case from yanchang formation, middle and Southern Ordos Basin, China. Petrol Explor Dev 37:543–551. https://doi.org/10.1016/S1876-3804(10)60054-7

Uguru CI, Onyeagoro OU, Sikiru IO (2002) Permeability modelling for reservoirs in the Niger Delta based on geological descriptions and core data, SIPM Rev Rep, 4:4–98

Wang F-R, He S, He Z-L et al (2009) Carbonate cements features and its genetic significance of sandstones in Yongjin Area of Junggar Basin. Acta Petrol et Mineralogica 28:169–178

Zhang M-Q, Huang S-J, Wu Z-X, Hu Z-W (2007) Carbonate cements and their formation mechanism in palaeogene sandstones of Lishui Sag, East China Sea Basin. J Chengdu Univ Technol (Sci Technol Ed), 34, 259–266

Zhang Y-W, Zeng J-H, Gao X, Zhou S-Y (2009) Distribution characteristics and main controlling factors of carbonate cements in the paleogene reservoirs in dongying depression. J Jilin Univ (Earth Sci Ed) 39:16–22

Zhu PY, You L, Yuan QT, Zhong J, Liu AQ (2018) Mechanism and distribution of calcareous interbeds in songtao uplift and its periphery of Qiongdongnan Basin. Open J Marine Sci 8:370–385